HUMMING NOISE MECHANISM IN AUTOMOTIVE BLOWER

Manuel HENNER, Aurélien SERRAN, Bruno DEMORY, Said NAJI,
Olivier CHERIAUX, Fabrice AILLOUD, Thibaud MATHARAN

Valeo Thermal Systems

8, rue Louis Lormand ZA de l'Agiot, La Verrière 78321, France

SUMMARY

In some circumstances, a spurious additional humming noise is observed in automotive blowers for HVACs units. This particular phenomenon can be easily identified in the acoustic spectrum with the evidence of wide peaks at the wheel rotational frequency and its harmonics. Several unsteady simulations have highlighted at low flow rate the effect of the recirculation at the top of the wheel which brings some vortical structures at blower entrance and which impacts the blade leading edges. Vortexes are spinning at low velocity inside the wheel, and are creating quasi periodic pressure fluctuations on wheel and scroll surfaces. Analysis done during tests and simulations confirm the relationship between the wide peaks and the vortex distributions.

INTRODUCTION

Automotive blowers for HVACS (heating, Venting and Air conditioning System) are highly constrained ventilation devices, mainly for the purpose of the integration in the dashboard which requires a good compactness. A typical HVACS is presented in figure 1, where one can see the various equipment yielding pressure losses: a quite common configuration requires two heat exchangers (a heater core and an evaporator for climate control), an air filter and several flaps aimed to redirect the flow in the different area of the cabin. For some obvious reasons of compactness and lightening, the cross section area inside the HVACS and all the piping connected to the diffusers are reduced to their bare minimum, with a limit fixed by the air velocity which should not exceed 15 m/s for acoustic reason. In addition, the air circuit includes a lot of turn, by-pass and variation of shape which create a high amount of pressure losses.

The blower must then compensate for increasingly higher pressure levels due to complexity of HVACS, driven by the demand for comfort (several areas in the cabin, addition of purifying filters) and the reduction of the space in the dashboard (more electronic devices).

The mass production imposes that the blower remains however quite conventional, and it consists of an assembly of a cylindrical wheel in a compact volute, as presented in figure 2, driven by an electrical motor of about 250 Watt. It is important to note that the wheel is made of plastic, and the respect of molding rules prohibits the presence of a reinforcing flat ring at the extremity of the blades. It is replaced by a lateral ring presented in figure 3 which ensures the rigidity of the wheel and which allows each of the blades to be freely extracted from the mold cavity.

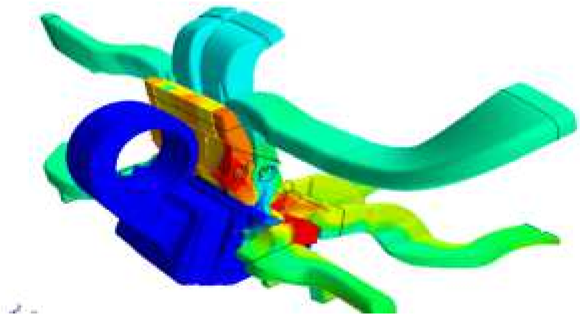

Figure 1: Automotive HVACS with venting ducts

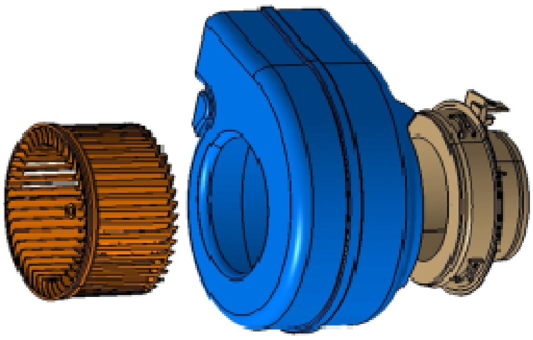

Figure 2: Blower wheel, volute and motor holder

The wheel is directly mounted on the electrical motor shaft, this later being placed in a motor holder which damps vibration by rubber plots. As a consequence of both the support flexibility (aimed to filter motor harmonics) and the tolerancing of plastic parts, an important tip clearance of about 4 mm is needed between the wheel and the entrance of the blower. This constraint is at the detrimental of both aerodynamics and aeroacoustics, and therefore some surfaces have been adapted to guide the air at the entrance and to limit effects of recirculation at blade tips. For instance, on the cross section of the tip clearance presented in figure 4, a wall aimed to produce a kind of labyrinth for the tip recirculation can be seen.

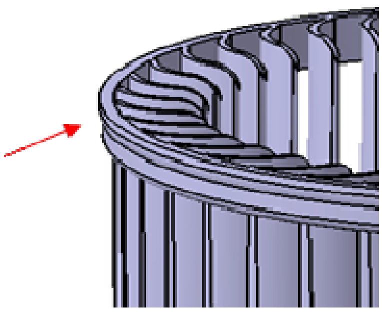

Figure 3: Details of the lateral ring on the wheel

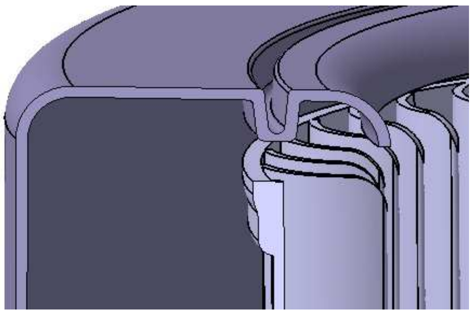

Figure 4: Details of the tip clearance between wheel and volute

BLOWER ACOUSTICS

The acoustic of the blower is an important criterion as it impacts directly the passengers' comfort in the cabin. The design of this radial fan is then driven by some rules which are aimed to limit as far as possible the different mechanisms of noise, and one important target is the reduction of the tonal noise. Peaks appear usually in the acoustic spectrum at the blade passage frequency and its harmonics (namely H41, H82, H123, etc. for the 41 blade wheel of this study), and it is now becoming affordable to make some assessments on their intensities by numerical means. The most classical method is using the FW&H theory [1], where the sources are computed by an unsteady simulation. Marsan & al have shown that the tonal noise for such a subsonic radial fan can be predicted quite accurately, preferably when using compressible schemes [2]. Such simulations are also helpful to analyze source location by using wall pressure spectra: it confirms that most of the tonal noise is produced by the interaction of the rotor with its surrounding, for instance with upstream struts like in the paper of Sanjose & al [3], or with downstream vanes as in the paper of Kelladi & al [4]. When a scroll is used, the most intense interaction occurs at the volute tongue, and is strongly dependant to its relative distance from the wheel and to its shape. As demonstrated by Velarde-Suárez & al [5] a smooth shape of the tongue is preferably used, as well as a span wise inclination aimed to create a phase shift between bottom and top of the wheel. It can be also noted that the recording of the pressure fluctuation at the tongue, either experimentally or numerically as done by Younsi & al [6], is therefore a good indicator for the assessment of acoustic trend during design phases.

The broadband noise for this subsonic case for which maximum Mach number is below 0.05 is mostly produced either by turbulence interaction with leading edges or by the turbulence in the boundary layers of blade suction sides. Several analytical models using this description based on Amiet’s theory [7] have been proposed by Roger & al [8], Kucukcoskun & al [9] or Moreau & al [10] for instance. However these models are somehow quite difficult to use for automotive radial blowers because the theoretical values from the airfoil theory cannot be found in a numerical flow analysis. Indeed separations on the blade suction are very important, as shown by Henner & al [11], and the contribution of the volute is not accounted for.

Therefore current industrial tools to predict broadband noise are either based on simplified models or on direct acoustic simulation with a Lattice Boltzmann method. In the first case, some self-similarities are used to compare blowers when their geometries are equivalent and when effects of size, power and rotational speeds are under investigation. This approach allows very fast analysis during the early phases of design, as presented by Naji & al [12]. It can be advantageously completed by a Lattice Boltzmann simulation at the cost of an intense CPU effort, and it can provide an acoustic spectrum which correlates quite well with experiment, as shown by Perrot & all [13].

HUMMING NOISE

In some circumstances, a spurious additional humming noise is observed in the system. This particular phenomenon is quite unpleasant and can be easily identified in the acoustic spectrum with the evidence of wide peaks at the wheel rotational frequency and its harmonics, as presented in figure 5. In this case, the blower wheel has a diameter of 150 mm, a height of 90 mm and was spinning at 3600 rpm. The operating point has a relatively low flow coefficient of 0.11, since its best efficiency is observed for 0.3.

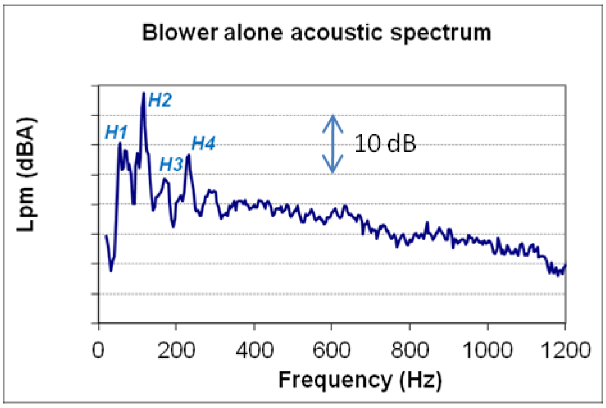

Figure 5: Acoustic spectra showing peaks (humming noise)

In worst cases, peaks can be 15 dB above the broadband level and the consequences are important since any usage of such blower is allowed. Not only the global noise increases by 2.5 dB (acoustic power), it also results in a production of a loud monotone note that test engineers name humming noise.

Conditions of occurrence of this unacceptable noise are not well understood so far, but available cases seem to point out the relationship between a low flow rate and an important recirculation at the top of the wheel. In order to better understand these unconventional cases, a study both experimental and numerical has been initiated.

EXPERIMENTAL TEST

The selected test case corresponds to the blower who produced the spectra of figure 5 and briefly described in the previous paragraph. Two simple tests are performed to compare the acoustic spectra with or without tip clearance recirculation:

- The classical configuration is tested at different flow rates. Tip clearance height is 4 mm, the standard lateral ring is present.
- The same blower with a modified tip arrangement is tested. The wheel has an additional flat ring at blade extremities, and the tip clearance is filled with foam (see figure 6). Recirculation is then removed, or at least reduced to a very low amount.
- The same blower with a trailing edge modification is tested as well. The main objective of this modification is to modify the flow exit angle by adding a sharp trailing edge (see figure 7).

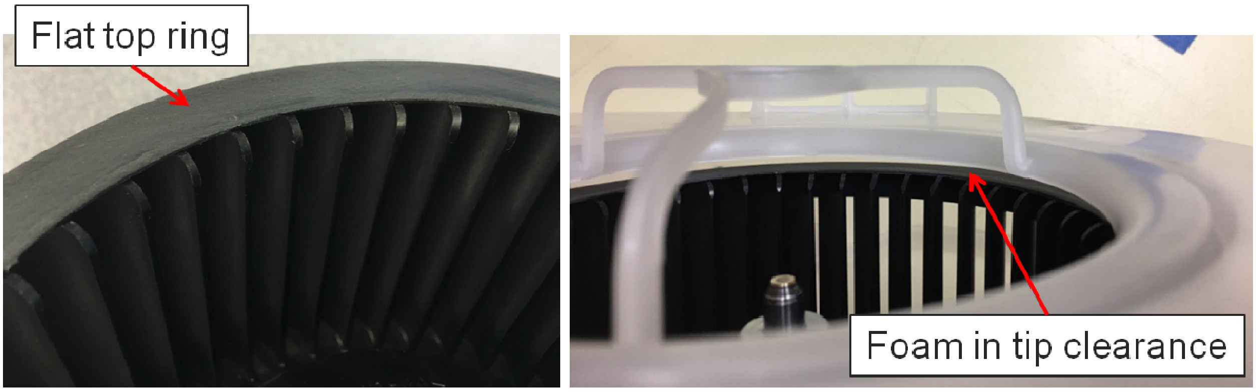

Figure 6: Tip clearance with flat ring and foam

Test rig description

Investigations are conducted on the test rig located in our R&D center in La Verriere (France), this latter being used for both aerodynamic performance measurements and for aeroacoustic characterization (see figure 8). The flow rate is set with different plates having calibrated holes which are placed at the outlet, its value being deduced from the pressure measurement according to the norm ISO 5801 [14]. Tests can be performed either with the blower driven by its own electrical motor, or by a torquemeter connected to an electrical motor with an extended shaft (one shaft termination hold the wheel, the second one is connected to the torquemeter). The rig is equipped with an anechoic termination, and 3 microphones with wind deflectors located in the outlet pipe are used to record the sound according to the norm NFS 31-063 (see figure 9). The bandwidth range is validated between 100 Hz to 2 kHz.

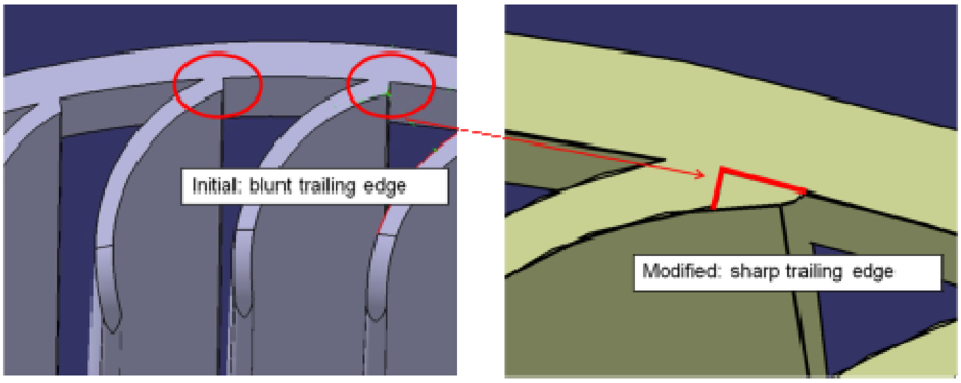

Figure 7: blade trailing edge modification.
Left: initial design with blunt trailing edge - Right: modified design with sharp trailing edge

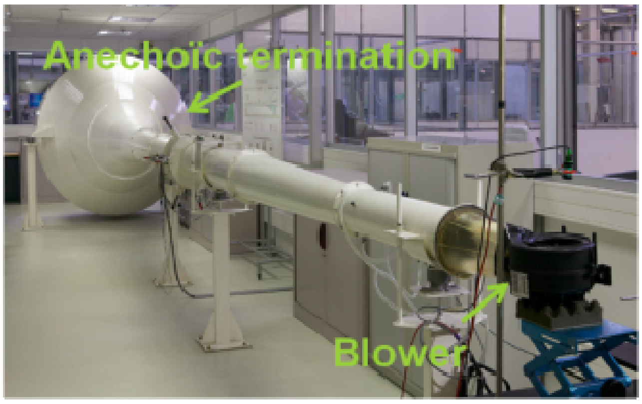

Figure 8: test rig facility at LVR

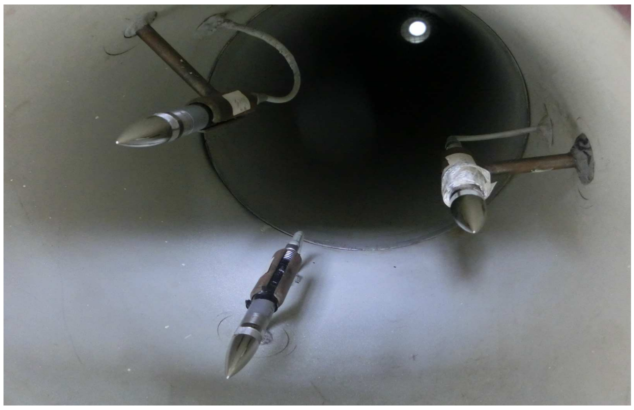

Figure 9: Microphone arrangement

Results

Aerodynamics performances were measured for the three configurations, and results are compared on the Δp-Q curves presented in figure 10. Very little differences are observed, especially for pressure curves that are very similar. Only the modified geometry creates a slight increase of pressure at high-flow rate, which can be explained by a bigger exit angle and consequently a little bit more tangential velocity (see paragraph with numerical simulation for details).

Surprisingly, closing the gap with the flat ring and the foam does not change the fan behavior, and the reduction of losses in the tip clearance has not produced the expected improvement. It must be reminded that the initial design was developed to sustain the tip recirculation, and the new arrangement may not be suitable for the current blade shape. In particular, the lateral ring shown in figure 3 is always present and constitutes an obstacle for the radial flow. In favor of this assumption, the static efficiency η shown in figure 11 demonstrates as well the decrease in efficiency when closing the blade to inlet housing gap.

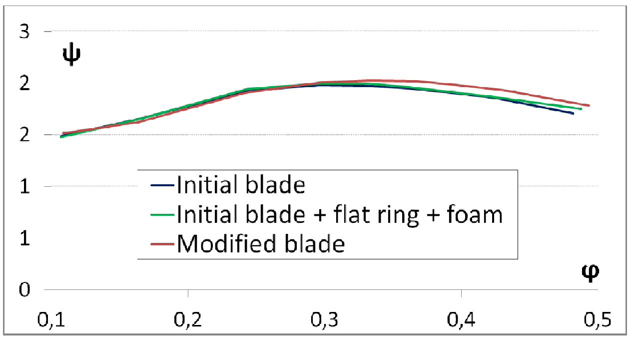

Figure 10: compared Δp-Q curves

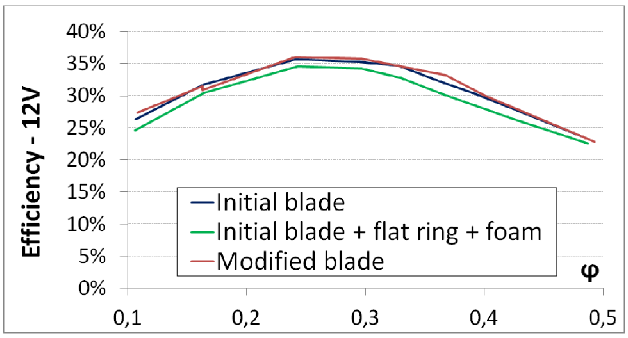

Figure 11: compared η-Q curves

Aeroacoustic performances are compared as well, at first in term of global sound pressure weighted with aerodynamic power, according to the formula $K_W = L_W - 10\log Q_V - 20\log \Delta P_t$, where Q_V and ΔP_t are respectively the volume flow rate and the pressure rise. Differences observed in figures 12 are this time much more important with strongly modified curves:

- when closing the tip clearance with foam, it is observed that noise is slightly reduced over a wide range of operating points, i.e. below flow coefficients of 0.35
- when modifying the trailing edge shape, noise is strongly reduced at very low flow coefficient (i.e. below 0.2), and becomes almost equivalent to the initial configuration after. It is also observed a slight degradation for the flow coefficient of 0.25, but it could be considered as rather negligible for this level.

These differences may indicate that several effects could trigger the noise production. By looking closely acoustic spectra in figure 13 for flow coefficient 0.14, several modifications in peak shape appears:

- when closing the tip clearance with foam, the most important peak close to H2 is significantly reduced (-7 dB), and the one close to H4 sees a reduction of 4 dBA. Unfortunately it is at the detrimental of another bump in the spectrum, i.e. the one close to H1 which increases by 4 dBA
- when modifying the trailing edge shape, all peaks are this time significantly reduced with respectively -3, -8, -3 and -4 dBA for bumps close to H1, H2, H3 and H4.

All in all, it can be announced that modifying the tip clearance can bring 1 dBA at low flow rate, whereas our modification on trailing edge brought 1 to 2 dBA bellow flow coefficient of 0.25.

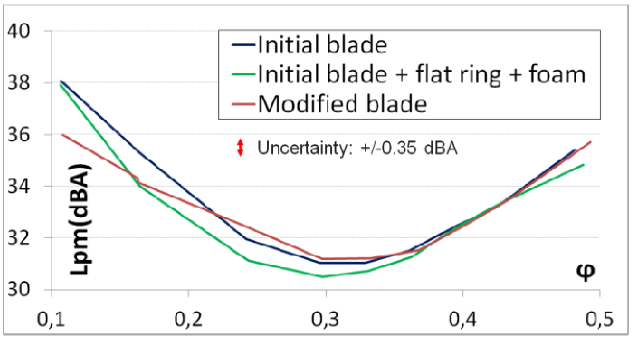

Figure 12: compared Kw-Q curves

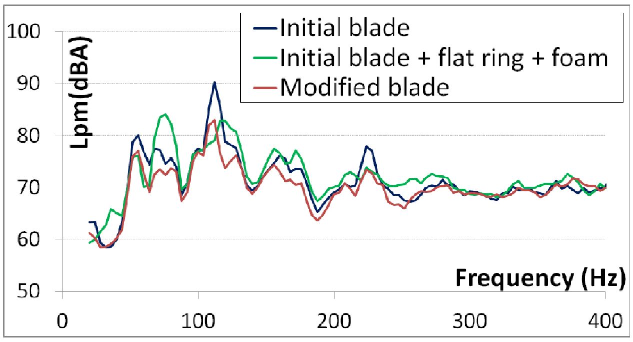

Figure 13: Acoustic spectra

NUMERICAL SIMULATION

Tests have shown that the tip clearance recirculation is causing this noise resulting in harmonic bumps in the frequency spectrum. A numerical study was initiated to understand that noise production mechanism.

Numerical model

The simulation domain has been meshed with 22 millions of polyhedral cells with the commercial code CCM+ from CD-adapco (figure 14). The exact geometry of the blower has been considered for this study, including the electrical motor which is cooled by an air recirculation loop (air is sucked at the connection behind the volute tongue, goes through the electrical motor and is pushed under the wheel hub). The simulation is carried out using the k-ω SST turbulence model and the two-layer model is used to predict accurately the boundary layer on walls. Y+ values on walls are mostly in range of 1 to 10 on the wheel and the volute. A moving reference frame is used to initiate the simulation in a steady mode, and then the unsteady simulation is performed with a time step of

~7e^{-5} s. 4 wheel rotations are needed to evacuate the numerical transition, and 4 additional wheel rotations are used for the recording of the various parameters post-processed.

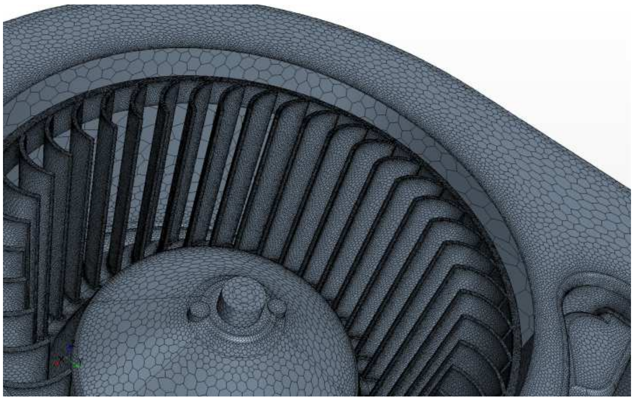

Figure 14: Overview of the mesh

Flow analysis

A first turbomachine analysis is performed by analyzing the two velocity components Vr (radial) and Vt (axial) at the wheel entrance and exit (these values are averaged both in time and circumferentially). Vr distributions along the wheel height show that most of the flow is going through the blade passage at mid span (figure 15). It can be noted however that the initial geometry sees some disturbance since its maximum radial velocity is located lower than for the two other geometries. Some recirculation effects in the tip will be presented later and could explain this difference. For the two other geometries, radial velocity profiles appear smoother, and even the one with foam sees smaller velocities. It is obviously the consequence of the tip clearance closing which avoids that an additional flow is being recycled permanently.

The tangential velocity distribution is presented in figure 16, showing identical behavior for initial geometry with or without foam. This is in line with the previous observation of their pressure curves which were also identical. The modified design produces a more important work since tangential velocities are bigger on the highest part of the wheel. This is probably due to a change of profile that has been slightly lengthened by the tip of the trailing edge, with a solid exit angle also slightly modified. At this flow rate, however, it does not allow to note a pressure increase on the performance curve of the figure 10. This tangential speed increase is probably wasted in the recirculation since Vt is already greater at the entrance of the wheel, on its highest part.

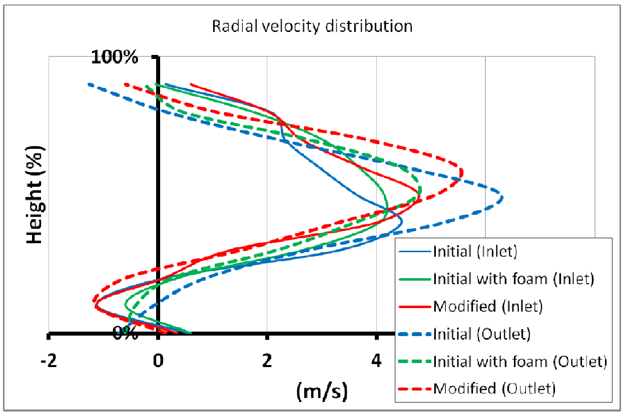

Figure 15: Vr distributions along the wheel height

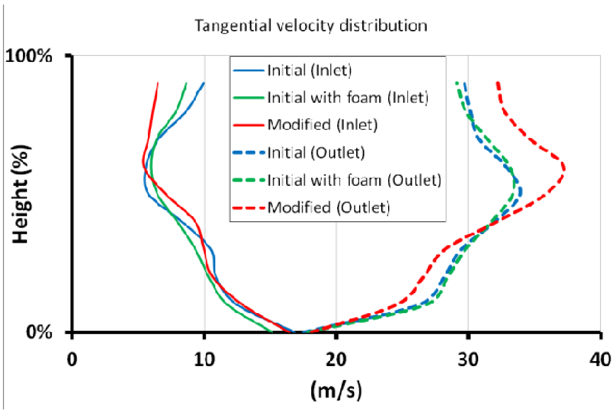

Figure 16: Vt distributions along the wheel height

The inlet velocity post-processing demonstrates that a significant pre-rotation of the flow occurs inside the wheel. This phenomenon has been observed from time and space averaged velocity distributions, and it points out the need for unsteady phenomenon analysis. A visualization of the vorticity shows that large swirl structures are created in the wheel and near the volute tongue (figure 17). These vortexes do not remain positioned in front of the tongue, but as they are trapped inside the wheel, they are spinning both on themselves (vorticity) and inside the wheel. As they move approximately at the wheel speed, they produce peak as for the tonal noise but at the frequency of passage in front of the volute tongue, not at the blade passage frequency. The relationship between the rotation frequency of the wheel and the structures is not yet clearly established, but a simulation over a longer period would have made possible to check if these frequencies correspond to the frequencies of the harmonic peaks in the acoustic spectral analysis. So far it can be just assumed that these peaks are wide because the rotating speed of the vortexes is not fixed and may vary.

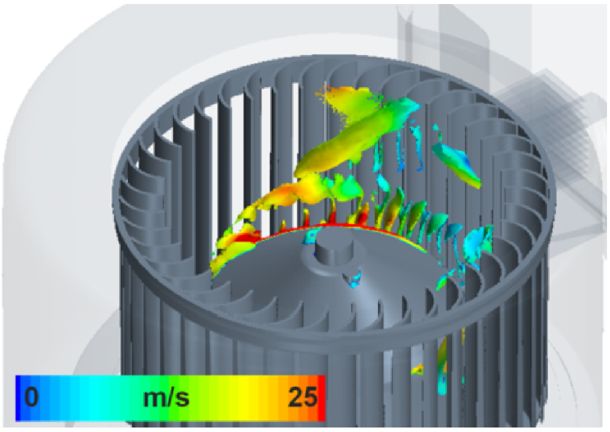

Figure 17: Isovorticity colored by relative velocity

It appears during this unsteady analysis that the structure originates in the close proximity of both the volute tongue and the tip clearance. In order to complete this observation, a focus is being done on the recirculation and its consequences in the scroll. A comparison between the 3 configurations is presented in figure 18 with a focus on the vortical structures that spin inside the volute. Their centers of rotation are pointed out with a red circle in order to highlight the greater distance at each modification, i.e. from the initial, the one with foam and lastly the modified. The main effect related to this observation is that the flow is less straight with the first design and it confirms the disturbance of the radial velocity suggested by Vr distribution in figure 15. The flow getting out of the blade to blade passage is finally more homogenous along the wheel height with the modified geometry, as suggested by the red arrows aligned with the stream lines.

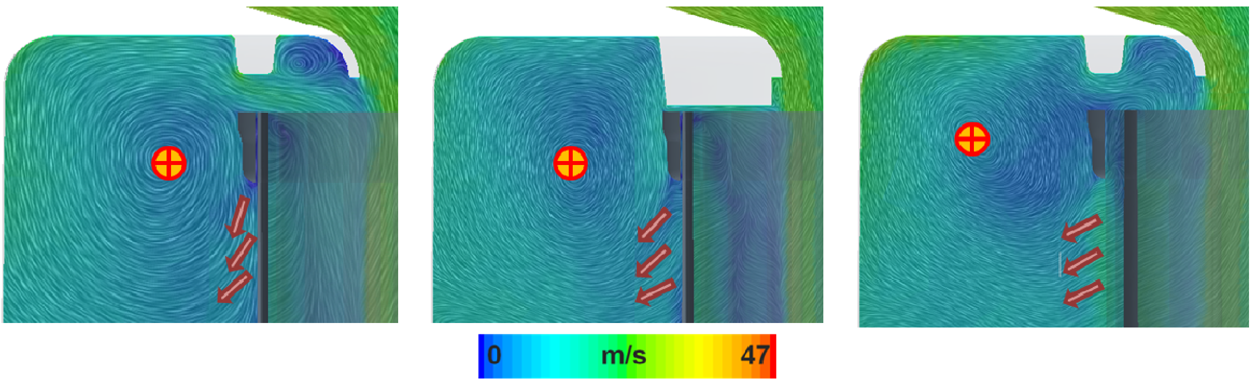

Figure 18: comparison of vortical structures inside the volute

Another phenomenon has to be highlighted with the velocity mapping inside blade to blade passages. The comparison presented in figure 19 is showing circumferential planes developed and colored by the velocity for the 3 geometries. The position of the tongue can be easily found by its trace with lower velocities and the acceleration it creates just before. It is still at this point just a qualitative analysis which however allows noticing a more homogeneous distribution with the modified wheel. Conversely, the initial wheel sees more structures in rotation, especially in the upper part, i.e. in the tip clearance in which one can observe small vortexes winding between the head of the wheel and the upper casing.

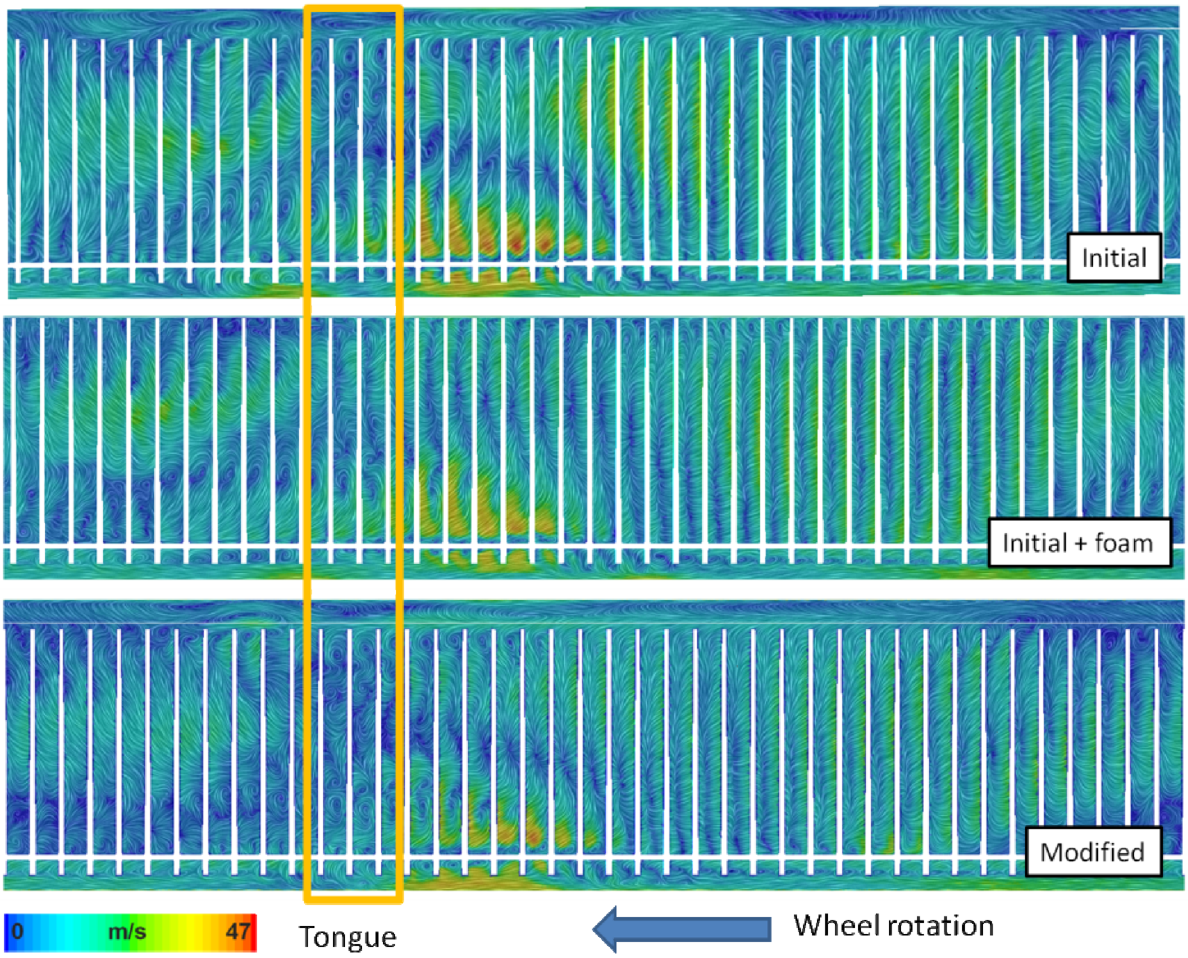

Figure 19: Velocity on a developed circumferential surface in the wheel

To establish the link between this observed unsteadiness in the flow and the acoustic spectrum, a search for dipolar sources was carried out by placing a series of probes along the volute tongue. Fourier transforms of temporal recordings of parietal pressure are presented in figure 20 for both the initial wheel and the modified wheel, from a sensor located at mid-span. Other signal comparisons have shown more or less the same 10 dB difference in sound pressure level on the wall. Of course it does not tell how this noise is propagated in the blower and in the far-field, but it is an additional argument to state that the observed unsteady phenomena are the origin of the bumps observed in the acoustic spectra.

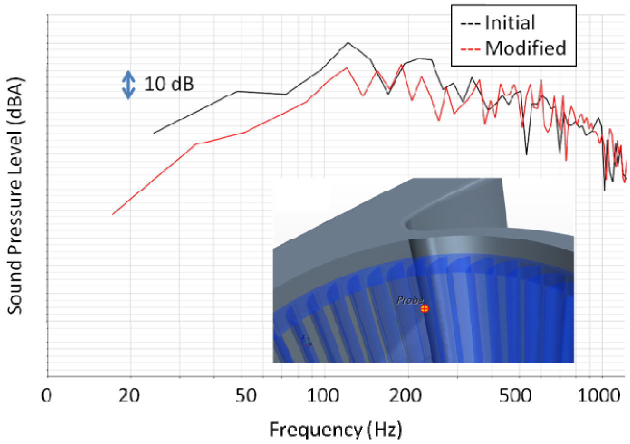

Figure 20: Fourier transforms of temporal recordings of parietal pressure

CONCLUSION

Experiments conducted were aimed to find some relevant parameters which can trigger the humming noise. Among them, the flow coefficient is obviously the most important as the phenomenon appears at low flow rate, when the tangential velocity becomes too important compared to the radial one. Therefore the compactness of automotive blower is unfortunately a favorable ground for this noise mechanism as the design leads to highly loaded wheels. Probably many different parameters may either delay or trigger the occurrence of the phenomena. For instance tests have shown the influence of the tip clearance recirculation or of the trailing edge angle; their effect has been further investigated thanks to fluid simulations which have shown that some vortical structures appear upstream of the blade. These structures are spinning approximately at the rotational speed of the wheel, this explaining that the bumps in the acoustic spectra are about the first four harmonics of the wheel rotation.

In order to avoid the occurrence of this phenomenon, future ventilator designs will take these phenomena into account, thanks to unsteady simulation which helps us to predict its apparition. The parameters to be taken into account will obviously be the flow rate, the filling of the fluid vein over the blade height and the homogeneity of the flow in the wheel entrance.

ACKNOWLEDGEMENTS

Authors would like to thanks Cyril Vincent-Viry for his help during simulation and post-processing.

BIBLIOGRAPHY

[1] Ffowcs Williams, J. & Hawkings, D. (**1969**), “Sound generation by turbulence and surfaces in arbitrary motion, Philosophical Transactions for the Royal Society of London”, A264: 321–342.

[2] Marsan A., Moreau S., “Aeroacoustic analysis of the tonal noise of a large-scale radial blower.”, ISROMAC 16, 16th International Symposium on Transport Phenomena and Dynamics of Rotating Machinery, April 10-15, **2016**, Honolulu

[3] Sanjose M., Moreau S., Gullbrand J., “Hybrid noise predictions of a radial notebook blower”, ISROMAC 16, 16th International Symposium on Transport Phenomena and Dynamics of Rotating Machinery, April 10-15, **2016**, Honolulu

[4] Khelladi S, Kouidri S, Bakir F, Rey R., "Predicting tonal noise from a high rotational speed centrifugal fan", Journal of Sound and Vibration 313/1-2:113–33, **2008**.

[5] Velarde-Suárez S., Ballesteros-Tajadura R., Santolaria-Morros C. and Pereiras-García B., "Reduction of the Aerodynamic Tonal Noise of a Forward-Curved Centrifugal Fan by Modification of the Volute Tongue Geometry", ASME 2005 Fluids Engineering Division Summer Meeting, Houston, Texas, USA, June 19–23, **2005**.

[6] Younsi M., Bakir F., Kouidri S. and Rey R., "Numerical and experimental study of unsteady flow in a centrifugal fan", Proc. Inst. Mech. Eng., Part A: J. Power Energy, 221(7):1025–1036, **2007**.

[7] Amiet R.K, "Acoustic radiation from an airfoil in a turbulent stream", Journal of Sound and Vibration 41(4), 407-420, **1975**

[8] Roger M. and Moreau S., "Extensions and limitations of analytical airfoil broadband noise models", International Journal of Acoustics 9(3), 273-305, **2010**.

[9] Kucukcoskun K., Christophe J., Schram C. and Tournour M., "Broadband scattering of the turbulence interaction noise of a stationary airfoil: experimental validation of a semi-analytical model", International Journal of Aeroacoustics, January **2013** vol. 12 no. 1-2 83-102.

[10] Moreau S. and Roger M., "Effect of Airfoil Aerodynamic Loading on Trailing Edge Noise Sources", AIAA Journal, Vol. 43, No. 1 (**2005**), pp. 41-52.

[11] Henner M., Demory B., Bonnet P.A., Tannoury E., Beddadi Y., "Automotive blower optimization using parameterized geometries and design of experiment", Annual Conference of the CFD Society of Canada (CFDS), May 6-9, **2013**, Sherbrooke, Canada.

[12] Naji S., Ailloud F., "Automotive HVAC unit noise prediction using blower dimensioning tool", International Conference Automobile and Railroad comfort, Le Mans France (**2008**), pp. 41-46.

[13] Pérot F., Kim M.S., Wada K., Norisada K., Kitada M., Hirayama S., Sakai M., Imahigasi S. and Sasaki N., "HVAC Blower Aeroacoustics Predictions Based on the Lattice Boltzmann Method", ASME-JSME-KSME Joint Fluids Engineering Conference, Hamamatsu, Japan, July 24–29, **2011**

[14] ISO standard DP 5801 – Industrial Fans – performance testing using standardized airways, **1997**.